# Molecular Imaging by Means of Multispectral Optoacoustic Tomography (MSOT)

Vasilis Ntziachristos* and Daniel Razansky

*Chair for Biological Imaging, Institute for Biological and Medical Imaging, Technische Universität München and Helmholtz Zentrum München, Munich, Germany*

*Received July 23, 2009*

## Contents



## 1. Introduction

Optical imaging is a powerful modality in biological discovery. The mainstream of optical interrogations, however, largely relies on microscopy, which imposes depth limitations on resolving novel classes of optical reporter agents developed for in vivo use, such as fluorescent proteins and probes, other chromophoric molecules, and nanoparticles with specificity to cellular and subcellular activity. We review herein emerging optoacoustic (also termed photoacoustic) technologies that allow the visualization of optical reporter agents with never-seen-before visualization performance, enabling volumetric quantitative molecular imaging in entire organs, small animals, or human tissues. Multiwavelength/multispectral optoacoustic (photoacoustic) methods, in particular, allow for highly specific molecular imaging through several millimeters to centimeters of tissue with resolutions in the 20−200 $\mu$m range, combining high contrast versatility with resolution that is largely independent from photon scattering in tissues. The principles of operation, key operational characteristics, and examples of *in vivo* imaging in fish and mice are described, showcasing performance that forecasts optoacoustic imaging as a method of choice for biological visualization and selected clinical segments.

Optical imaging operates on contrast mechanisms that offer highly versatile ability to visualize cellular and subcellular function and structure. Correspondingly, fluorescence microscopy and imaging are overwhelmingly utilized in biomedical research, for example in immunohistochemistry, in vitro assays, or cellular imaging *in vivo*. The compelling advantages of fluorescence are reflected in the recent development of powerful classes of fluorescent tags that can stain functional and molecular processes in vivo. A widely acknowledged technology is the 2008 Nobel-prize awarded *fluorescent protein*, which offers perhaps the most versatile tool for biological imaging.[1] Fluorescent proteins are reporter molecules that attain the ability to tag cellular motility and subcellular processes, from gene expression and signaling pathways to protein function and interactions, merging optimally with postgenomic "-omics" investigations and interrogating biology at the systems level. Promising new developments include the introduction of truly near-infrared shifted FPs, with excitation and emission spectra above 650 nm.[2] Such performance opens exciting possibilities for whole body animal imaging, as it allows high sensitivity imaging through several centimeters of tissue, due to the low photon attenuation by tissue in the 650−950 nm range, i.e. the near-infrared (NIR) spectral region. In parallel, a plethora of extrinsically administered probes are being developed, also operating in the NIR region.[3,4] Fluorescent probes are optical reporter agents that can probe tissue constituents and their function by staining *in vivo* certain classes of cells, receptors, proteases, and other moieties of cellular or subcellular activity. During the past decade, a large number of experimental and commercially available fluorescent agents is increasingly offered, from fluorescent dyes with preferential accumulation to tissues of interest to activatable photoproteins and fluorogenic-substrate-sensitive fluorochromes[3] with molecular specificity. Collectively, these developments offer a highly potent toolbox for biological imaging.[5] So far, these contrast mechanisms were proven efficient in a number of small-animal applications, but many of these agents attain strong potential for clinical translation as well. In addition, voltage sensitive dyes, fluorescence resonance energy transfer approaches, and lifetime measurements further allow the sensing of ions, protein−protein interactions, or the effects of the biochemical environment on the fluorochrome.[6,7] Using fluorescence therefore, previously invisible processes associated with tissue and disease growth and treatment can be sensed and visualized in real-time and longitudinally. Naturally, fluorescence is widely used in basic biological discovery and drug discovery, and it is even considered for clinical studies of cancer and inflammation and neurodegenerative and cardiovascular disease, to name a few examples.

Other chromophoric, nonfluorescent, assays and agents have also been considered as read-out techniques of expression patterns or protein activity, for example the encoding of $\beta$-galactosidase as a reporter molecule[8,9] or the use of chropmophoric substrates for monitoring enzymatic activity.[10]

* Corresponding author. E-mail: v.ntziachristos@tum.de.

10.1021/cr9002566 
Published on Web 04/14/2010

Vasilis Ntziachristos, Ph.D., is a Professor and Chair for Biological Imaging at the Technische Univestitat Munchen and the Helmholtz Zentrum Munchen and the Director of the Institute for Biological and Medical Imaging. Prior to this appointment he served as Instructor and Assistant Professor at Harvard University and the Massachusetts General Hospital. He received his masters and doctorate degrees from the Bioengineering Department of the University of Pennsylvania and the Diploma on Electrical Engineering from the Aristotle University of Thessaloniki, Greece. His main research interests involve optical and optoacoustic imaging methods and their application to postgenomic preclinical and clinical challenges.

Daniel Razansky obtained his Ph.D. in Biomedical Engineering and his M.Sc. and B.Sc. degrees in Electrical Engineering, all from the Technion—Israel Institute of Technology. Following postdoctoral research at the Harvard Medical School and the Massachusetts General Hospital, he was appointed to the Faculty of the Institute for Biological and Medical Imaging (IBMI), Technische Univestitat Munchen and the Helmholtz Zentrum Munchen. Currently, he serves as the Head of the Experimental Biological Imaging Systems Laboratory and Deputy Director of IBMI. His research interests include development of novel molecular imaging and contrast approaches using multispectral optoacoustics and mesoscopic optical imaging techniques.

In addition, different nanoparticles with optical contrast, such as gold or carbon nanoparticles, can be functionalized for targeting specific cells and cellular structures and considered for molecular imaging applications.[11−14]

In-vivo imaging of optical reporter agents is typically achieved in cell monolayers or thin tissue slices using conventional microscopy techniques. In the past two decades, significant progress has been achieved by developing and using confocal and multiphoton microscopy to image deeper in tissues.[15,16] By offering technology that can account for photon scattering in tissues, confocal microscopy can reach depths of up to 100−200 $\mu$m when imaging highly scattering tissues *in vivo*, and two-photon and multiphoton microscopy can penetrate 300−500 $\mu$m. While these depths have yielded unparalleled insights into *in vivo* cellular function, they usually do not allow sampling of entire structures—for example, entire tumors—or visualize organs and events that are not superficial. Optical projection tomography (OPT)[17] and selective plane illumination microscopy (SPIM),[18] developed recently as alternative volumetric imaging methods to confocal and nonlinear microscopy, are also strongly limited by tissue scattering. These techniques are ideally suited for volumetric imaging of low-scattering samples, but they typically cannot penetrate as deep as two-photon microscopy when it comes to highly scattering tissue imaging *in vivo*.

Imaging deeper than a few hundred micrometers is possible, especially when utilizing optical reporter agents that operate in the near-infrared (NIR), whereby detection through several centimeters in tissues can be achieved. This is because of the low light absorption by tissue in the far-red and near-infrared regions (650−900 nm). Imaging, however, through several millimeters to centimeters of tissue is significantly complicated by the photon scattering process in tissues, which contributes to a significant resolution loss. Scattering also limits the quantification ability when imaging at depths beyond a few hundred micrometers. In response, *macroscopic* optical tomography was considered for quantitatively resolving optical contrast in three-dimensions.[19] Optical tomography utilizes optical measurements through multiple illumination and detection paths (projections) around the tissue of interest[20] and mathematically combines these measurements to reconstruct three-dimensional images of the optical contrast inside the object imaged. Optical tomography methods significantly improved the ability to resolve and quantify activity situated deep in tissues, over two-dimensional photographic approaches originally considered for macroscopic optical imaging of entire animals or human tissues.[19,20] More recently, significant betterment in macroscopic optical imaging performance comes from hybrid approaches, including optoacoustic (also termed photoacoustic) methods[21] or the combination of optical tomography with high resolution methods such as X-ray computed tomography (CT)[22,23] or magnetic resonance imaging (MRI).[24] Compared to stand-alone optical imaging and tomography methods, hybrid methods offer significant advantages in the imaging performance achieved and are emerging as important and highly versatile tools for visualizing tissue biomarkers in biological discovery and potentially in select clinical applications.

Optical imaging methods that can tomographically image fluorochrome biodistribution by detecting the emitted fluorescence have been reviewed.[25] Instead, herein we focus on the use of optoacoustics for optical molecular imaging applications at depths that go beyond the ones achieved by optical microscopy. We discuss the basics of multispectral optoacoustic technology and its use to detect tissue biomarkers, followed by representative applications from *in vivo* imaging of different optical molecular probes. The operational characteristics of the method are also discussed and offer predictions on the future development of the field of molecular optoacoustic imaging. Optoacoustic imaging can further capitalize on the distinct optical spectra that some tissue elements attain, for example hemoglobin, and it has also been considered for imaging of intrinsic tissue contrast, for example the distribution of blood vessels or blood oxygenation; for these latter applications, the interested reader can refer to excellent recent publications on this subject.[26,27]

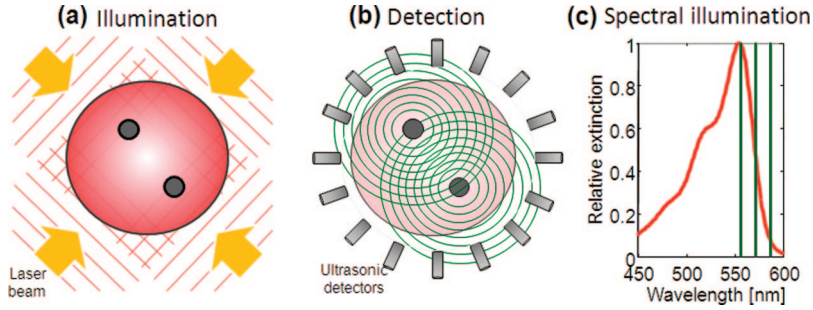


**Figure 1.** Principle of MSOT operation. (a) Pulsed light of time-shared multiple wavelengths illuminates the tissue of interest and establishes transient photon fields in tissue. (b) In response to the fast absorption transients by tissue elements, acoustic responses are generated via the thermoacoustic phenomenon, which are then detected with acoustic detectors. By modeling photon and acoustic propagation in tissues and using inversion (tomographic) methods, images can then be generated and spectrally unmixed to yield the biodistribution of reporter molecules and tissue biomarkers. (c) Light of different wavelengths (green lined) is selected to target the absorption transient of the chromophore or fluorochrome, as selected for spectral differentiation; here shown with the absorption spectrum of the fluorescent protein DsRed2 (red line).

## 2. Principle of Operation

Optoacoustic imaging is based on the generation of acoustic waves following the absorption of light pulses of ultrashort duration. The optoacoustic (or photoacoustic) phenomenon has been known for more than a century,[28] but its utilization for biomedical applications, such as spectroscopy or imaging, has been considered in the past decades,[29−31] further intensifying in the past few years. By combining now commercially available pulsed laser technology in the nanosecond range and sensitive acoustic detectors, it was shown possible to generate optoacoustic responses from tissue and visualize subsurface blood vessels with high resolution.[21]

While hemoglobin within subsurface blood vessels can be detected in single wavelength images, volumetric imaging of photoabsorbing agents typically requires differentiation of these agents on top of spectrally varying background absorption, due to intrinsic tissue photoabsorbers such as hemoglobin and melanin, other chromophores, lipids, and water. In response, multispectral optoacoustic tomography (MSOT) relies on the spectral identification of chromophoric molecules and particles distributed in tissue over background tissue absorption. The MSOT principle of operation is shown in the sample experiment of Figure 1, where tissue is illuminated with light pulses of duration in the 1−100 ns range. Pulses of different wavelengths are used, in a time-shared fashion, whereas the wavelengths are selected to sample a spectral characteristic in the absorption spectrum of the reporter agent of interest, as shown, for example, in Figure 1c for the fluorescent protein DsRed2. In response to the fast absorption of light pulses by photoabsorbing agents, the latter undergo a thermoelastic expansion that emits mechanical waves at ultrasonic frequencies. These waves can then be detected by acoustic detectors placed in proximity to the illuminated tissue. Using appropriate mathematical methods, images of the absorbed energy can then be reconstructed in analogy to the formation of ultrasound images or X-ray CT images. The amplitude of the generated broadband ultrasound waves depends on the optical absorption properties. The spatial resolution of the method is therefore determined by the diffraction limit of ultrasound waves or the available bandwidth and geometrical characteristics of the ultrasonic detector.

While images can be generated for each light wavelength separately, multiwavelength illumination and spectral processing are necessary for identifying the unique spectral signatures of optical reporter agents of interest in the presence of intrinsic tissue chromophores. Agents with absorption spectra that have characteristic differences from the absorption of background tissue are best suited for MSOT imaging. In particular, molecules or nanoparticles with steep absorption changes are optimal for MSOT imaging, since they can then be resolved by scanning narrow spectral bands. The simplest form of spectral processing is the subtraction between images obtained at two adjacent wavelengths under the assumption that tissue will have a similar absorption at these wavelengths and its effects will cancel out the background absorption and bring out the distribution of the reporter agent and the corresponding tissue biomarker. This concept has been shown to work in optically homogeneous phantoms[32] but its *in vivo* use may be problematic, since tissues are generally heterogeneous and the tissue absorption also generally has a distinct spectral profile. In this case, the use of more sophisticated spectral processing methods that can separate the spectral signature of reporter agents from that of background absorption may be necessary, especially when baseline measurements are not possible.[33] By employing scanning at different spectral bands, multiple chromophoric molecules or nanoparticles can be resolved during the same imaging session.

As reviewed in section 5, reporter agents with molecular specificity without characteristic spectral signatures can also be optoacoustically detected using single wavelength measurements, for example, agents with slow varying, broad absorption spectra. Such detection, however, relies on the availability of baseline measurements, i.e. images obtained before the appearance of the agent, and are typically appropriate for strongly absorbing agents with fast distribution or expression dynamics.

For accurately operating *in vivo* and in a volumetric fashion, MSOT further needs to account for light propagation in tissues, essentially therefore accounting for the effects of intrinsic tissue optical properties (absorption and scattering) on photon distribution. This is because each pixel in the raw optoacoustic image is the product of tissue absorption at that pixel times the local photon energy deposited. While superficial optoacoustic imaging[21] in the first few hundred micrometers of propagation can assume a piecewise homogeneous distribution of light in tissues and generate meaningful images, optoacoustic signals generated from deep tissue regions do not accurately reflect the underlining optical absorption but rather the combined effect of tissue absorption

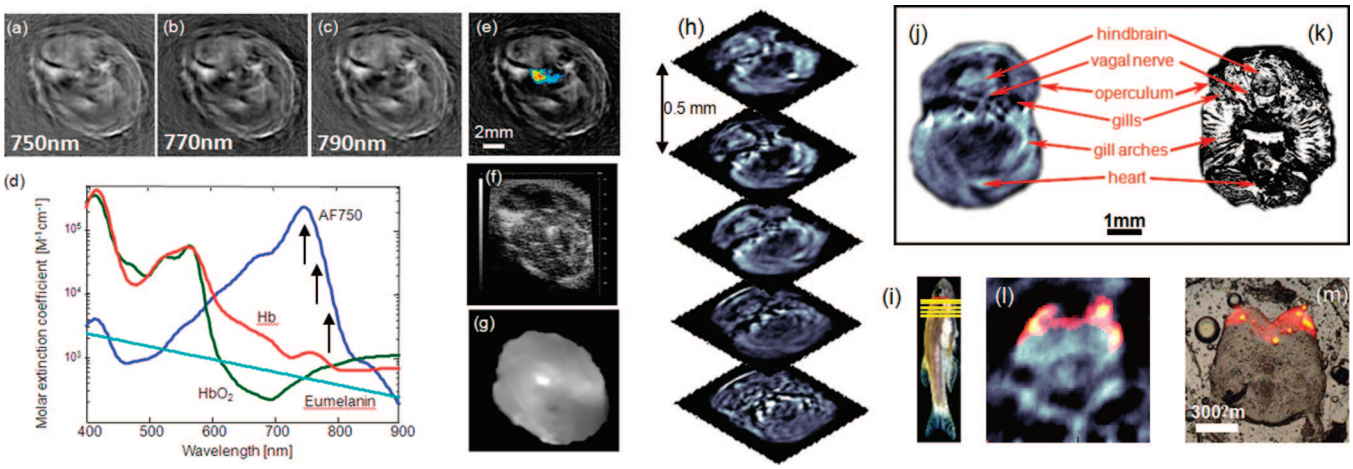


**Figure 2.** (a−g) Multispectral optoacoustic tomography (MSOT) visualizes the distribution of a fluorescent molecular probe (AlexaFluor 750) in a mouse leg.[33] (a−c) Cross-sectional optoacoustic tomographic reconstructions acquired at 750, 770, and 790 nm, respectively. (d) Absorption as a function of wavelength for an AF750 fluorescent probe as compared to some intrinsic tissue chromophores. Arrows indicate the three wavelengths used to spectrally resolve the probe location. (e) Spectrally resolved MSOT image that incorporates measurements at all the three indicated wavelengths (in color), superimposed onto a single-wavelength anatomical image. (f) Corresponding ultrasonic image, acquired approximately at the same imaging plane, using a 25 MHz high-resolution ultrasound system. (g) Planar epifluorescence image of dissected tissue, confirming the fluorochrome location. (h−m) Three-dimensional *in vivo* imaging through the brain of an adult (6 months old) mCherry-expressing transgenic zebrafish.[35] (h) Five cross-sectional optoacoustic imaging slices through the hindbrain area (i) of living zebrafish taken at 585 nm. Example of imaged slice and its corresponding histological section are shown in parts j and k, respectively. (l) MSOT image of the brain (zoom-in) with mCherry expression shown in color. (m) Corresponding epifluorescence histology made through an excised brain.

and light distribution. Unprocessed single wavelength images may therefore offer details that can be identified as certain tissue structures, but typically these may not be quantitatively accurate unless adequately processed. Therefore, a significant aspect of MSOT technology is the use of appropriate methods that decompose the effects of photon distribution from spatial changes of optical absorption in order to yield accurate and quantitative images of optical reporter agents in tissues, as described in more detail in the section "Quantification Challenges" that follows.

In summary therefore, there are two basic components required for quantitative molecular optoacoustic imaging of optical reporter agents in tissues:

1. Multispectral separation is necessary in order to distinguish with specificity the agent's spectral signature over the nonspecific background absorption. Preferred photoabsorbing agents in this case have distinct spectra compared to the background absorption spectrum. Fluorescent proteins, organic dyes, and fluorochromes and different nanoparticles, such as gold nanorods, for example, attain this characteristic by offering spectrally narrow extinction (absorption) spectra that can further enable multispectral detection of multiple spectrally separated agents.

2. Accounting for the effects of light propagation in tissues in order to decompose the true probe concentration from variations of the optoacoustic signal due to light intensity variations in tissue is also necessary.

## 3. In-Vivo Imaging Using MSOT

The MSOT ability to detect reporter molecules in tissues has been so far showcased by visualizing fluorochromes and fluorescent proteins in mice, fish, and other biologically relevant organisms. Parts a−g of Figure 2 depict results from ref 33 resolving a common organic fluorochrome (AlexaFluor 750) injected in a mouse leg. Parts a−c of Figure 2 depict cross-sectional optoacoustic tomographic reconstructions acquired at single wavelengths of 750, 770, and 790 nm, revealing an excellent morphological contrast from an intact leg. Figure 2e shows an MSOT image (in color), generated by spectral processing of Figure 2a−c superimposed onto Figure 2b (gray scale). Figure 2f depicts a corresponding ultrasonic image (25 MHz transducer) whereas Figure 2g shows a planar epifluorescence image of the dissected tissue that confirms the fluorochrome location, as was noninvasively revealed by MSOT in Figure 2e. In a similar manner, the method was used to visualize glioblastoma tumor cells stereotactically implanted into mouse brain with the help of IRDye800-c(KRGDf) agent.[34] As discussed, MSOT operates optimally by selecting optical reporter agents with a steep drop in their absorption spectrum or otherwise a distinct spectral signature over tissue background absorption, as shown in Figure 2d. The characteristics of agents, such as gold nanoparticles and fluorochromes that are of appropriate spectral characteristics, are more analytically reviewed together with other optical reporter agents in section 5.

High resolution deep tissue imaging of fluorescent proteins (FP) by MSOT was also recently demonstrated,[35] which may enable useful applications in MSOT imaging of gene expression. Parts h−m of Figure 2 show results from whole-body visualization of deep-seated fluorescent proteins expressed in mature diffuse organisms with high (mesoscopic) resolution (in this study 38 $\mu$m), while simultaneously providing the necessary reference anatomical images. The images were three-dimensionally (3D) acquired *in vivo* through the brain of an adult (6 months old) mCherry-expressing transgenic Zebrafish with a cross-sectional diameter of around 6 mm. The results demonstrate the ability to reveal high-resolution molecular activity and superimpose it onto morphological features of identical resolution in the brain of an intact living animal.

One important consideration in the *in vivo* MSOT use regards laser safety. Currently, the maximal permissible exposure (MPE) for human skin is set by the American National Standards Institute (ANSI) to 20 mJ/cm$^2$ for single

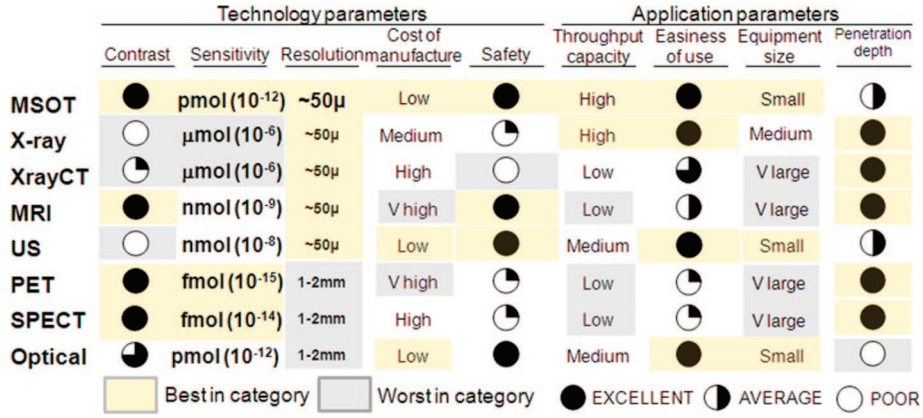


**Figure 3.** MSOT performance versus other imaging modalities.

nanosecond pulse exposure in the 400−700 nm visible range.[36] This limit is gradually raised through the near-infrared toward 100 mJ/cm$^2$ at 1050 nm. However, tomographic optoacoustic application may involve repetitive illumination of the region of interest, in which case also the average power deposition exposure limits have to be met, namely 200 mW/cm$^2$ in the visible, gradually increasing to 1 W/cm$^2$ at 1050 nm in the near-infrared. The recent molecular imaging results shown in animals[35] were within these safety recommendations and point to a corresponding performance when considering clinical translation as well.

## 4. Overview of Performance Characteristics

A particular strength of optoacoustic imaging is the ability to simultaneously deliver anatomical, functional, and molecular contrast from tissues using a single modality, a characteristic that is otherwise typically achieved using a combination of multiple modalities.[37] Optoacoustic technology scales well with different tissue sizes, especially when employing near-infrared light. Indeed, its range of operation begins at depths where two-photon microscopy ends (~0.5−1 mm), achieving resolutions in the sub 20 $\mu$m range,[38] and can visualize specimens of several centimeters in size (diameter) with resolutions in the range of 100 $\mu$m.[39] The limits of penetration of the technique depend on the ability to deposit sufficient photon energy in tissues, a property that in turn depends on the tissue's optical properties, that absorb and scatter light, reducing its strength as a function of propagation distance. Typically, small animal imaging dimensions are possible, but larger organs, such as the whole human breast[40] and primate brain,[41] have also been visualized. Similarly to ultrasound, optoacoustics is an inherently fast imaging technology;[42] therefore, it holds great potential for real-time imaging of fast events and dynamic processes, such as pharmacokinetics, in living organisms.

Based on the performance showcased in recent studies, multispectral optoacoustic tomography offers revolutionary performance, i.e. high resolution and sensitivity, very versatile molecular contrast, portability, scalability, cost effectiveness, and the use of nonionizing radiation, as summarized in Figure 3. While the existing imaging modalities attain some of these features, *none combines all of them in one package*, as in MSOT. The major limitation of MSOT over many other modalities is the penetration (sensitivity as a function of depth) that can be achieved due to the strong light attenuation in tissues. As a result, MSOT is expected to become a method of choice in small animal imaging research. When considering clinical applications, MSOT has several niche focus points due to the high sensitivity, resolution, and portability, and it can shift the paradigm of healthcare, offering a safe point-of-care imaging modality for highly disseminated imaging. Foreseen application areas are all the endoscopic areas, where compared to similar photographic/color imaging, it can impart superior quantification and offer high resolution in-depth imaging in three dimensions as well. In addition, breast imaging,[43] joint imaging,[44] and vascular imaging[45] (either intravascular or noninvasive) are all within the performance capacity of the method. Correspondingly, MSOT is expected to enter focused segments of the therapeutic efficacy and possibly the diagnostic segments, especially in areas not well served by current imaging modalities. Therefore, its application segment does not compete with the MRI and PET application areas but defines new operational fields that are more closely associated with traditional clinical segments utilizing optical imaging but offering significantly more powerful and informative performance in resolving tissue and disease biomarkers. MSOT is seen as highly complementary to established radiology and nuclear imaging modalities but also to conventional optoacoustic methods developed for anatomical and functional imaging.

## 5. Contrast Approaches and Reporter Agents

In living mammalian tissues, strongly absorbing endogenous chromophores such as melanin or oxy- and deoxyhemoglobin may by themselves be used to form images (for example of blood vessels or of melanoma cells) but they also impose challenges when imaging other intrinsic or extrinsically administered nanoparticles, since they then contribute to an undesirable background. Consequently, compounds with high molar extinction (absorption) coefficients that can be detected above this intrinsic tissue optoacoustic signal are important for molecular imaging applications.[46] From a molecular imaging perspective, efficient optical reporter agents are essential, since normal and diseased tissues and cells cannot easily be distinguished *in vivo* using endogenous chromophores.

Due to high plasmonic absorption in the near-infrared and visible spectra, gold-based agents have been extensively explored in recent years and were shown to increase optoacoustic signals *ex-vivo* and in living tissues. Rayavarupu et al. evaluated gold nanoparticles conjugated with monoclonal antibodies specific to HER2 overexpressing SKBR3 for possible detection of breast carcinoma cells.[12] Gold nanorods were detected with high sensitivity *in vivo*[13] and later conjugated with Etanercept and used for *ex-vivo*

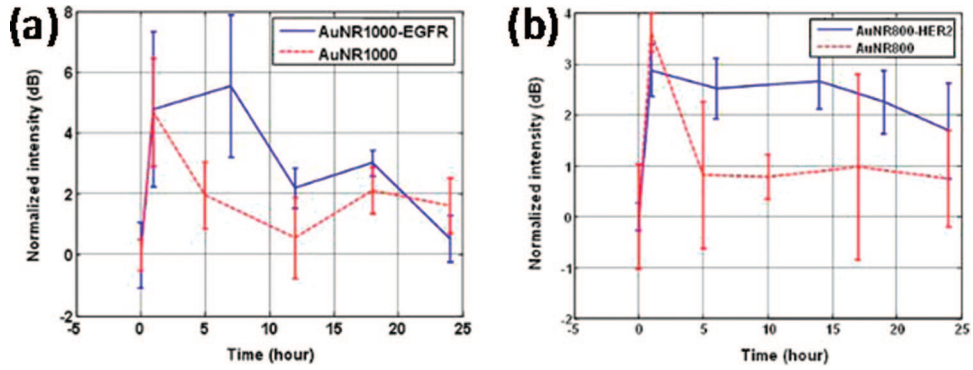


**Figure 4.** *In-vivo* optoacoustic imaging of subcutaneous squamous cell carcinomas in mice with tumor-targeting gold nanorods. (a) Averaged optoacoustic image intensities within the tumor region versus time after injection of EGFR-targeting (solid line) versus untargeted (dashed line) nanorods. (b) Averaged image intensities within the tumor region versus time after injection of HER2-targeting (solid line) versus untargeted (dashed line) nanorods. The averages were calculated from three cross-sectional images. Error bars indicate standard deviations. Reprinted with permission from ref 11. Copyright 2008 Optical Society of America.

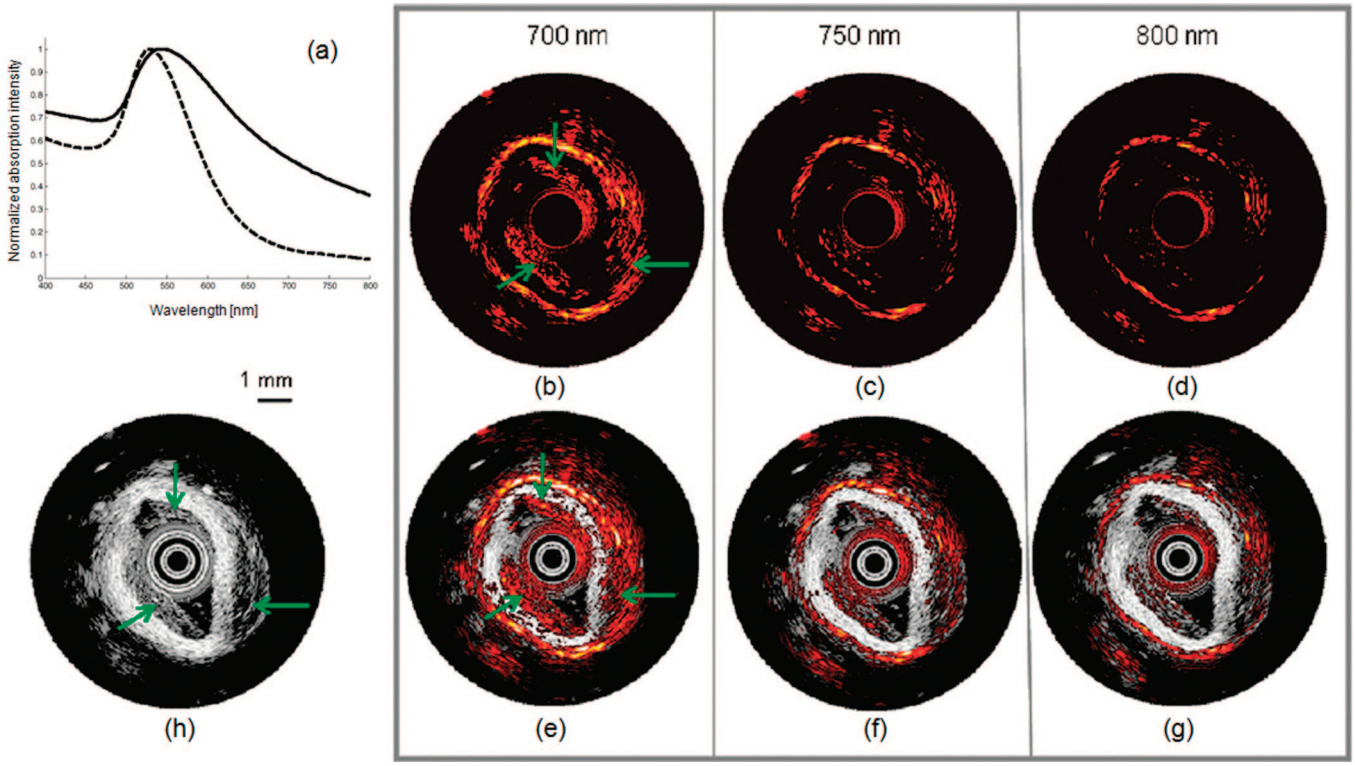


**Figure 5.** Multispectral optoacoustic detection of macrophages in atherosclerotic plaques using an absorption spectrum shift of plasmonic gold (Au) nanoparticles (NP). (a) Normalized extinction spectra of macrophages loaded with Au NPs (solid line), and Au NPs only (dashed line). Both absorption spectra were normalized with their corresponding maxima. Panels b−h show intravascular ultrasound (IVUS), intravascular photoacoustic (IVPA), and combined IVUS/IVPA images of a diseased rabbit aorta injected with macrophages loaded with Au NPs. The IVUS image is displayed in part b using a 50 dB dynamic range. The injected macrophages in the outer and inner regions of the aorta are denoted in parts b, c, and f with green arrows. The normalized IVPA images (c−e) and combined IVUS/IVPA images (f−h) obtained using 700, 750, and 800 nm wavelengths are displayed using a 20 dB display dynamic range. The IVPA and combined IVUS/IVPA images taken at 700 nm wavelength (c−f) showed a high photoacoustic signal at the injected regions denoted by arrows. Reprinted with permission from ref 45. Copyright 2009 American Chemical Society.

monitoring of anti-TNF drug delivery.[47] Gold nanorods conjugated with anti-HER2 and anti-EFGR have been used for targeted optoacoustic imaging of OECM1 and Cal27 squamous cell carcinomas both *in vitro* and *in vivo*.[11] As compared to the baseline measurements made before the probe's injection, contrast enhancement of up to 10 and 3.5 dB, respectively, was reported (Figure 4). Gold nanoparticles, in particular those shaped into rods, shells, cages, etc., can be generally engineered to attain distinct spectra so that they can be detectable by MSOT or used in single wavelength studies to visualize fast dynamic phenomema, typically in physiology studies. Alternatively, one can capitalize on the absorption spectrum shifts due to specific uptake of the nanoparticles by, for example, cells or macrophages. For instance, Wang et al.[45] demonstrated that intravascular photoacoustic imaging can assess the macrophage-mediated aggregation of nanoparticles and, therefore, identify the presence and the location of nanoparticles associated with macrophage-rich atherosclerotic plaques (Figure 5).

Other nanoparticulate agents were shown to enhance contrast in optoacoustic imaging studies. A recent longitudinal study has demonstrated that single-walled carbon nanotubes (SWNT) conjugated with cyclic Arg-Gly-Asp (RGD) peptides can be used as a contrast agent for

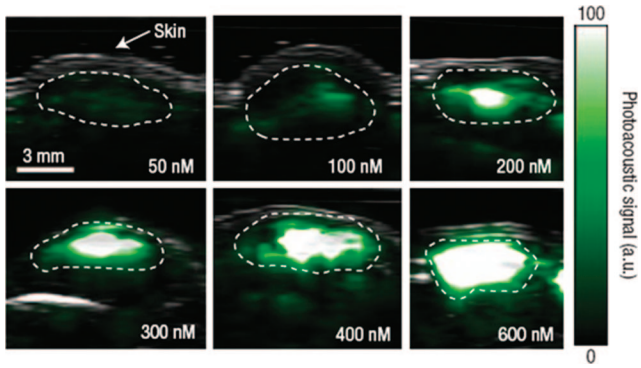


**Figure 6.** Optoacoustic detection of RGD-conjugated single-walled carbon nanotubes in tumor-bearing living mice. Mice were injected subcutaneously with single-walled carbon nanotubes at concentrations of 50−600 nM. One vertical slice in the 3D optoacoustic image (green) was overlaid on the corresponding slice in the ultrasound image (gray). The skin is visible in the ultrasound images, and the optoacoustic images show the single-walled carbon nanotubes. The dotted lines on the images identify the edges of each inclusion. Reprinted with permission from ref 14. Copyright 2008 Macmillan Publishers Ltd.

optoacoustic imaging of tumors.[14] Intravenous administration of these targeted nanotubes into mice bearing tumors showed an eight times greater optoacoustic signal in the tumor in comparison to mice injected with nontargeted nanotubes (Figure 6). An enzyme-activated chromogenic assay was used in optoacoustic tomography by Li et al.[48] with LacZ gene encoding for the X-gal chromogenic substrate. Shashkov et al. suggested using conjugated quantum dots as multimodal contrast agents for integrated fluorescent, photothermal, and photoacoustic detection and imaging.[49,50] Fluorochromes and organic dyes can also serve as reporter molecules, as reviewed in section 3. Furthermore, agents used in other nonoptical imaging modalities, such as MRI, can potentially be used for creating contrast in optoacoustics and as multimodal agents.[51] Table 1 provides representative characteristics of common optoacoustic contrast agents. While some physical and chemical parameters may greatly vary among different types of compounds, as far as is concerned with optoacoustic signal generation, a more accurate estimate of a contrast agent's efficiency can be obtained via the concentration-normalized absorptivity measured in $cm^{-1}/(mg/mL)$. This value represents the optical absorption coefficient (in $cm^{-1}$) one can create in the target volume by using a 1 mg/mL concentration of the contrast agent. For instance, while carbon and gold nanoparticles might generally have very high molar extinction values, these particles are also relatively large and heavy compared to other contrast molecules. Thus, after normalizing by molecular weight, some organic dyes (e.g., AlexaFluor 750) will have an even higher concentration-normalized absorptivity. Yet, the question of overall performance of various agents in targeted molecular imaging applications need to be evaluated in view of additional important parameters, such as targeting efficiency, binding capacity and target concentration on a per-cell or receptor basis.

When using fluorescent dyes for optoacoustic imaging, emphasis is given to low quantum-yield fluorochromes with high absorption cross sections, which are particularly useful for optoacoustic signal excitation. Conveniently for optoacoustics, many NIR fluorochromes possess relatively high molar extinction coefficients in excess of $10^5\ M^{-1}\ cm^{-1}$, in conjunction with low quantum yield (reduced fluorescence efficiency), acting in favor of optoacoustic signal generation. Many organic fluorochromes exhibit sharp resonances in the vicinity of their peak excitation, making them also spectrally attractive for MSOT applications. The absorption spectrum of AF750 that was employed in the example shown in Figure 2d drops significantly in the spectral window 750−790 nm, compared to the smooth absorption change of background tissue in the NIR. Therefore, intrinsic tissue contrast can be readily suppressed with a multispectral approach, yielding highly sensitive imaging of fluorochrome distribution in tissue obtained by spectral matching of optoacoustic images acquired at several different adjacent wavelengths.

Even though many other dedicated contrast agents could potentially be developed for optoacoustic imaging applications, long-term studies may be necessary for examining a variety of efficiency, dosing, safety, and toxicity aspects associated with biological discovery applications or the clinical translation of new contrast agents.[52] In this context, imaging of common fluorescent agents with clinical approval may be an immediately viable option for clinical MSOT. Overall, however, and while fluorochromes offer significant utility advantages, it would be ideal to focus on photoab-

**Table 1. Chemical and Optical Characteristics of Major Tissue Chromophores and Some Optoacoustic Molecular Contrast Agents[a]**

| chromophore | excitation wavelength (nm) | molar extinction coefficient[b] ($cm^{-1}\ M^{-1}$) | fluorescence quantum yield QY (%) | typical length of a single particle/ molecule (nm) | molecular weight[b] (g/mol) | concentration- and QY-normalized absorptivity[c] ($cm^{-1}/(mg/mL)$) | ref |
|---|---|---|---|---|---|---|---|
| oxygenated hemoglobin ($HbO_2$) | 750 | 520 | 0 | 6.8 | $6.4 \times 10^4$ | 0.008 | 33 |
| | 550 | $58 \times 10^3$ | 0 | | | 0.9 | 33 |
| eumelanin | 750 | 470 | 0 | 1 | 208 | 2.3 | 33 |
| | 550 | 1200 | 0 | | | 5.8 | 33 |
| near-infrared organic dyes (AlexaFluor750) | 750 | $2.5 \times 10^5$ | 12 | 2 | 1300 | 169 | 33 |
| red-shifted fluorescent protein (mCherry) | 587 | $7.2 \times 10^4$ | 22 | 5 | $2.6 \times 10^4$ | 2.2 | 35 |
| single-walled carbon nanotubes | 750 | $1.5 \times 10^7$ | 0 | 100 | $10^5$ | 150 | 14 |
| gold nanorods | 750 | $9.4 \times 10^8$ | 0 | 35 | $1.3 \times 10^7$ | 72 | 13 |
| activated chromogenic assay (X-gal) | 650 | $10^4$ | 0 | 1 | 408.6 | 24.5 | 48 |
| near-infrared quantum dots | 840 | $5 \times 10^6$ | 13 | 20 | $4.4 \times 10^5$ | 9.9 | 50 |

[a] The actual characteristics may vary depending on the particular compound and its functionalization; therefore, representative examples are provided. [b] The numbers are provided per particle/molecule. [c] Optical absorption coefficient in $cm^{-1}$, created in the target volume by a 1 mg/mL concentration of the contrast agent.

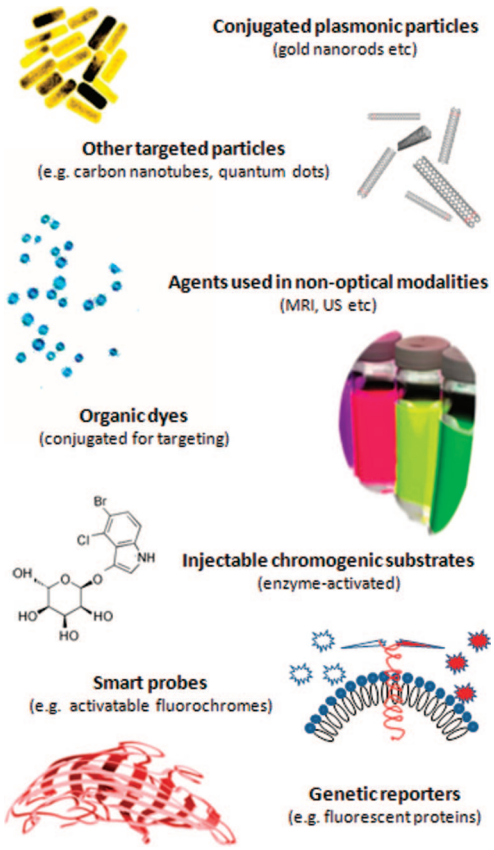


**Figure 7.** Molecular agents for MSOT and other optoacoustic imaging implementations.

sorbing reporter agents of low toxicity and high extinction coefficient to yield strong optoacoustic signals, while retaining distinct spectral profiles, so that they can be detected also in the absence of background (baseline) measurements, unless very fast biodistribution and targeting capacity can be imparted. Figure 7 summarizes the main types of molecular probes and markers currently available for MSOT and optoacoustic molecular imaging in general.

## 6. Other Optoacoustic Imaging and Sensing Techniques

A variety of optoacoustic imaging techniques are evolving as highly versatile methods from both application and technological standpoints. While this review is particularly concerned with the molecular imaging potential of optoacoustics, as it is enabled by multispectral methods, we briefly mention in this section some key areas of development that hold particular additional interest for the field.

The development of optoacoustic (photoacoustic) microscopy methods creates an alternative high resolution visualization method of tissues. By utilizing high frequency focused detectors, photoacoustic microscopy (PAM) has attained high fidelity volumetric images of *in vivo* vascular anatomy, oxygen saturation, blood oxygenation, and tumor neovascularization with spatial resolutions in the range of a few micrometers to a few tens of micrometers for millimeter-range penetration without introduction of contrast agents.[53] More recently, optical resolution photoacoustic microscopy (OR-PAM) demonstrated microvasculature images with single capillary resolution of several micrometers at limited penetration depths (up to 0.7 mm), revealing vasomotion and vasodilation effects noninvasively due to switching between

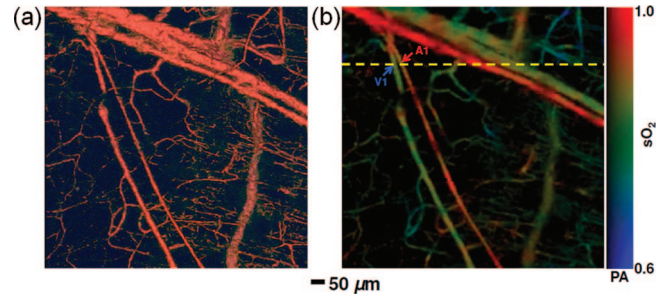


**Figure 8.** Structural and functional microvascular imaging by OR-PAM in a nude mouse ear *in vivo*. (a) Structural image acquired at 570 nm. (b) Vessel-by-vessel $sO_2$ mapping based on dual wavelength (570 and 578 nm) measurements. The calculated $sO_2$ values are shown in the color bar. PA: photoacoustic signal amplitude. A1: a representative arteriole. V1: a representative venule. Reprinted with permission from ref 54. Copyright 2009 Optical Society of America.

systemic hyperoxia and hypoxia[54] (Figure 8). By utilizing multispectral principles, the optoacoustic microscopy approach could be similarly utilized for molecular imaging applications.

At depths of a few hundred micrometers to a few millimeters, optoacoustic imaging of vascularization has been applied to imaging animal models of cancer[38] and cardiovascular imaging,[55] lymph node mapping,[56] detection of neurodegenerative disease,[57] or ocular imaging.[58] Initial feasibility studies in larger animals and humans are also available, such as breast tumor detection[43] and imaging of the brain,[41] peripheral joints,[44] skin vasculature,[38] and port-wine stains.[59] Even though blood provides the strongest intrinsic contrast for optoacoustic signal generation, optoacoustic tomography was also shown to be capable of attaining clear anatomical images from other tissues such as fat and bones.[60] This opens new possibilities for deep tissue optoacoustic imaging of structures and model organisms having low or otherwise no hemoglobin-based contrast, such as small insects, fishes, and worms.

Many directions are building up also around optoacoustic biosensing applications. Optoacoustic signals are intrinsically sensitive to various mechanistic properties of tissue and, therefore, can potentially be used for, for example, noninvasive temperature monitoring during hyperthermic or ablation treatments.[61] Another fascinating application, optoacoustic flow cytometry,[62] is used for detection and selective destruction of circulating tumor cells—a common marker for the development of metastasis. Here gold and carbon nanoparticles, targeted to tumor receptors, are used to increase the sensitivity and specificity of the method.[63] This review is however focused on molecular imaging applications of optoacoustics; therefore, biosensing is clearly beyond its scope.

## 7. MSOT Technology Components

In the following two sections, we review in more detail the fundamental mathematics and technology aspects required for MSOT image formation and quantification for the interested reader. The vast majority of biomedical optoacoustic imaging applications employ intense pulsed laser sources, even though other methods of optoacoustic signal generation exist, e.g. using modulated continuous wave sources.[64] After the acoustic wave is created by light absorption, its magnitude is proportional to the local light intensity, optical absorption coefficient, and thermoelastic

properties of the imaged tissue. The induced acoustic wave spectrum is mainly dependent upon the spatial frequency of the optical absorption variations and duration of the light pulse. For laser pulse durations in the nanosecond range, a biologically relevant spectrum of optoacoustically induced signals is usually of ultrawide-band nature with useful information contained in the ultrasonic spectrum between several hundreds of kilohertz and several tenths of megahertz.

For imaging or sensing purposes, ultrasonic detectors are placed in the vicinity of the imaged object as shown in Figure 1. Similarly to ultrasonic imaging, optoacoustics is a time-resolved method; that is, the time of arrival of the pressure wave directly indicates the distance to the optoacoustic source in the imaged object. If the detector is placed in position $\vec{r}'$, it will sense an integrated pressure wave, namely[65]

$$p(\vec{r}', t) = \frac{\beta}{4\pi C}\int_V \frac{\partial H(\vec{r}, t')}{\partial t'}\frac{d^3\vec{r}}{|\vec{r} - \vec{r}'|}\Bigg|_{t'=t-|\vec{r}-\vec{r}'|/v_s} \quad (1)$$

where the spatiotemporal distribution of the instantaneous power absorption density $H(\vec{r},t')$ is measured in [W/m$^3$] and is proportional to the product between local light intensity $U$ and optical absorption coefficient $\mu_a$; $\beta$ is the isobaric thermal expansion coefficient, which describes the relative increase of the tissue volume per temperature increase under constant pressure (isobaric condition); $v_s$ is the speed of sound in tissue; and $C$ is the specific heat capacity at constant pressure, describing the energy required by a unit tissue mass to raise its temperature by a temperature unit. The typical parameters for biological tissue are $\beta = 3 \times 10^{-4}$ [°C$^{-1}$], $v_s = 1500$ [m s$^{-1}$], and $C = 4.186$ [J g$^{-1}$ °C$^{-1}$]. Equation 1 can be interpreted such that, for each time point, the detected pressure variation has been created by integration over all the optoacoustic sources located on a spherical shell of radius $|\vec{r} - \vec{r}'|$ surrounding the detector point $\vec{r}'$. The shape of the optoacoustic signal created by an absorber depends on its size and optical absorption properties.[65]

The ultimate goal of optoacoustic tomographic imaging is the reconstruction of the underlining optical absorption contrast from a set of measured ultrasonic pressures $p(\vec{r}',t)$. Optical absorption can then be directly related to concentrations of intrinsic tissue chromophores and other biomarkers of interest. Often, focused detectors are used in order to reduce the dimension of the image reconstruction problem. For instance, in the case of a spherically focused acoustic detector, the detected waveforms directly represent the distribution of optical absorbers along the focus line, the so-called A-scan.[38] To obtain a 2D or 3D reconstruction, the detector is simply scanned along the object, or alternatively, beam-forming with phased arrays is employed. Likewise, cylindrically focused detectors reduce the reconstruction problem into two dimensions,[39] in which case tomographic inversion is necessary. Back-projection algorithms have been so far widely used for image reconstruction in optoacoustic tomography. These algorithms are based on approximate closed-form inversion formulas expressed in two or three dimensions and are analogues to the Radon transform. Back-projection formulas exist for several detection geometries and are implemented either in the spatiotemporal domain[32] or in the Fourier domain.[66]

The optical reporter agent(s) of interest can be resolved by using multiwavelength illumination, at different spectral bands for multiple agents, and subsequent spectral matching[33,35] of an a-priori known spectrum. To achieve this, in the simplest form, it is assumed that every pixel in a single-wavelength optoacoustic image represents a combined contribution of the photoabsorber of interest with known molar extinction spectrum $\alpha_b$ and unknown concentration $c_b$ and other background chromophores with known spectra $\alpha_m$ and unknown concentrations $c_m$ ($m = 1, ..., M$). This can be written in the form of a linear equation system, i.e.

$$\mu_a(\lambda_n) = \alpha_b(\lambda_n)c_b + \sum_{m=1}^{M}\alpha_m(\lambda_n)c_m, n = 1, ..., N \quad (2)$$

where imaging is performed at $N$ discrete excitation wavelengths. Using the measured absorption values and known spectra, the distribution of the optical reporter agent of interest can be subsequently reconstructed from the above linear equations on a per-pixel basis with, for example, a linear regression method. In order for this approach to work accurately, methods are required that impart quantification or that are insensitive to errors in the single wavelength images. The retrieval of images that reflect the true absorption values of the optical reporter agents of interest and are independent of the particulars of the photon distribution in tissue is therefore an essential aspect of MSOT, as described in the following section.

## 8. Quantification Challenges

Accurate evaluation of biomarker distribution, disease state, and treatment efficacy requires accurate quantification of biodistribution of the optical reporter agents utilized. Most existing optoacoustic imaging methods rely on explicit (closed-form analytical) back-projection reconstruction algorithms. These inversion methods are generally convenient and fast but are not exact and may lead to the appearance of substantial artifacts in the reconstructed images. A common problem in back-projection methods is the suppression of slowly varying image components and the accentuation of fast changes in the image (small details), which is usually also accompanied by negative optical absorption values that otherwise have no physical interpretation. In addition, back-projection algorithms are based on an ideal description of the acoustic wave propagation and detection as well as on specific detection geometries; therefore, they cannot be easily generalized into more realistic optoacoustic illumination−detection models that incorporate configuration- and instrumentation-dependent factors. The accentuation of fast changes often leads to high-resolution appearing images, but these images, especially when reconstructing complex distributed patterns, may lack significant accuracy.[67] The effects of acoustic and optical heterogeneities may introduce additional inaccuracies and image artifacts. For instance, acoustic speed variations in various tissues lead to dispersion and reverberation of optoacoustic signals. In the presence of large air cavities, such as lungs, the tomographic reconstruction can be therefore severely distorted. Moreover, in volumetric tissue imaging, the effects of light attenuation may cause the optoacoustic image to significantly deviate from the true absorption distribution, especially in response to the generally unknown spatially varying scattering tissue properties.[68] Consequently, the initially reconstructed optoacoustic image cannot be used to extract the optical absorption $\mu_a$ of the reporter agent used, which represents the biomarker distribution of interest. Therefore, even though the mentioned

reconstruction artifacts have not prevented nonquantitative structural imaging, they can significantly limit the utility of optoacoustics for molecular imaging applications and other types of longitudinal imaging studies that require accurate quantification. In the following, we address some of these issues for outlining the key progress in this matter.

It has been shown that optoacoustic image performance can generally be improved using the so-called model-based inverse methods[69] over back-projection algorithms. In contrast to backprojection algorithms, model based methods are not based on an approximate analytical solution of the optoacoustic equation. Instead, the forward problem is solved numerically. Iterative inversion algorithms have been suggested, whereby in each iteration the reconstructed optoacoustic image is changed to reduce the error between its corresponding acoustic signals and the measured signals. Ideally, this approach can yield artifact-free quantified reconstructions. However, the computational complexity involved with model-based schemes has so far severely limited their achievable resolution. Recently, a semianalytical model-based inversion scheme that has been considered for quantitative optoacoustic image reconstruction was suggested,[67] where the presented semianalytical solution is exact for piecewise planar acoustic-source functions, which significantly improves the accuracy and computational speed. The method eliminates image artifacts associated with the approximated back-projection formulations; that is, no negative absorption values are produced and the reconstructed image corresponds to the true light attenuation and energy deposition within the object. Model-based frameworks admit generalization of the forward solution to a more comprehensive acoustic propagation model without changing the inversion procedure. For instance, the frequency response of the acoustic detector as well as additional linear effects, such as the frequency dependent acoustic attenuation and the detector's focusing characteristics, can also be conveniently and rigorously incorporated into the model. Finally and importantly, the model-based inversion can be seamlessly adapted to any detection geometry.

Another quantification challenge arises from the fact that optoacoustic signals do not directly convey information on the underlining optical absorption coefficient $\mu_a$ but rather on the local power absorption density $H$ in tissue, which represents the product between $\mu_a$ and the local light fluence $U$. In cases of uniform sample illumination, e.g. in cases of superficial imaging,[21] where the light intensity can be nearly uniformly distributed over the imaged volume, the optoacoustic image is approximately proportional to the optical absorption coefficient. In practice, biological tissues present a highly heterogeneous environment with unknown optical properties therefore sample illumination can be rarely done in a uniform manner. For instance, when absorbing targets deeper in tissue are to be imaged, as in whole-body animal or organ imaging, the photon fluence is significantly attenuated as a function of depth and is also significantly affected by tissue optical heterogeneity. Optoacoustic images that are obtained using the assumption of uniform illumination will therefore be biased in favor of targets closer to the surface. Thus, in order to accurately reconstruct the object's absorption coefficient map, the light intensity within the tissue should be known so that it can be corrected for. Unfortunately, the light distribution depends on the precise map of tissue optical properties, which cannot be easily measured or calculated.

Cox et al.[70] suggested a simple iterative reconstruction algorithm for the planar geometry that can possibly resolve this imaging problem. In this algorithm, the optical absorption coefficient, obtained at each iteration, is used to calculate the fluence in the succeeding iteration. Theoretical simulations have shown that, under ideal conditions, the algorithm converges and accurately recovers the absorption coefficient. However, recent experimental findings indicate that while iterative inversion schemes can potentially improve image quality in optoacoustic tomographic imaging, their implementation needs to consider certain poorly known experimental factors that relate to the ability of accurately calculating the photon fluence distribution in the imaged object.[68] In particular, knowledge of the absorption and reduced scattering coefficient is not always available or straightforward to obtain. While the absorption coefficient can be directly linked to the optoacoustic signals, determination of the scattering coefficient is problematic, as no accurate method exists to volumetrically determine its distribution, especially when it is spatially varying within tissue. Even with exact knowledge of the optical properties, however, it was found that the iterative method did not yield convergence at long iterations and was rather influenced by different inconsistencies between experiment and theory, including noise and artifacts that can also be amplified.[68] Therefore, for the best performance in realistic imaging scenarios, iterative algorithms should preferably be used with some approximate or a-priori information on the imaged object, including a well-defined convergence criterion and a good estimate of the background optical properties.

A more advanced method for light attenuation correction relies on the general properties of the optical fluence, rather than the specific light-propagation model. The method sparsely decomposes the optoacoustic image into two components: a slowly varying global component attributed to the diffusive photon fluence in the medium and a localized high spatial frequency component representing variations of the absorption coefficient.[71] This decomposition is based on the assumption that, owing to light diffusion, the photon fluence exhibits a slowly varying spatial dependence in contrast to fast spatial variations of the absorption coefficient, more typically associated with variations in structures that have well-defined boundaries that introduce high spatial frequency components. The sparse representation of the optoacoustic image in the library directly yields both the quantitative map of the optical absorption coefficient and the light fluence.[71]

Finally, and in clear distinction to single wavelength imaging, MSOT can capitalize on the availability of multiple, potentially densely packed wavelengths and utilize a subset of this spectral information to improve quantification. The underlying premise is that the photon distribution in tissues is not expected to vary significantly for closely spaced wavelengths, especially in the near-infrared window. Therefore, measurements (images) at one wavelength can be explicitly used to normalize for photon intensity heterogeneity in tissues at the other wavelengths or, implicitly, during the spectral processing of the images. Such methods contribute to making MSOT approaches more robust and quantitative, especially in volumetric imaging applications.

## 9. Sensitivity of Biomarker Detection

While the feasibility of different optoacoustic imaging implementations has been showcased and initial predictions

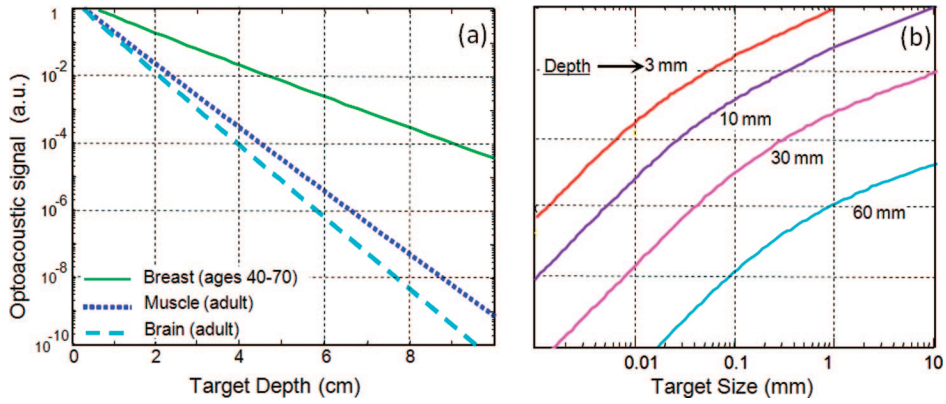


**Figure 9.** Simulated optoacoustic signal strengths from an experimental and clinical point of view.[65] (a) Optoacoustic response (on arbitrary scale) detected from a 2 mm diameter target containing a 1 $\mu$M concentration of a molecular probe (Cy5.5) at increasing depths of media mimicking various human tissues. Simulations were performed assuming tissue properties at a wavelength of 675 nm. (b) Signal variation versus target size.

have been reported in the literature on their sensitivity,[32−34] such predictions typically rely on, for example, a small set of experimental measurements and may not systematically capture true performance metrics. Moreover, the determination of the optoacoustic imaging sensitivity is not straightforward from a technical perspective, especially since the relation of sensitivity with volume and depth is not linear in optoacoustics. This is because volumes of different size generate optoacoustic responses of different spectral content, yielding different signal attenuation with depth due to frequency-dependent attenuation (dispersion) of sound in tissues. Light attenuation effects with depth can also produce nonlinear dependencies between the sensitivity and depth.

Since the optoacoustic resolution is generally high, the experimental determination of the sensitivity as a function of e.g. optical reporter agent volume remains difficult since this would require reproducible creation of small volumes (e.g., in the nanoliter range or less) containing well-defined concentrations of optical agents. A prediction can alternatively be made by imaging larger amounts of the same optical reporter agent and placing the measured value on a theoretically calculated signal intensity curve, calculated as a function of depth, or lesion size and limited by the noise floor of a particular system. A sensitivity estimate of a particular measuring device can then be made.[65] Figure 9 shows a practical example of such approach, as it examines the dependence of the detected optoacoustic signal upon target volume and depth for a typical organic fluorochrome (Cy5.5) with peak extinction at 675 nm. The prediction was obtained from simulations of optoacoustic signals emanating from a target probe, the latter represented by an absorbing sphere embedded at different depths in tissue-mimicking scattering and absorbing media.[65] As it can be observed, while optoacoustic signals depend linearly on concentration, they exhibit a nonlinear dependence not only as a function of target depth but also as a function of its volume. It is seen for example that for small targets (in practice, less than 0.2−0.5 mm in size), the effects of ultrasonic dispersion start playing an increasingly dominant role in the reduction of the detected optoacoustic signal intensity, owing to increased attenuation of high frequency sound components (Figure 9b). Therefore, for small targets sized less than 0.1 mm, signal reduction may become proportional to the third power of the target size, i.e. $d^3$. This finding demonstrates that it would be inaccurate to linearly extrapolate the detection limits of optoacoustics from data obtained on larger amounts of optical agent, but instead use an estimation model on detection limits that accounts for all effect of light attenuation and frequency dependent ultrasonic dispersion.

Overall, recent *in vivo* and phantom studies predicted detection limits in the subpicomole range for common fluorochromes in the near-infrared[39,65] and about one thousand cells for cells efficiently labeled with red-shifted fluorescent protein.[35] However, in cases of shallow depth imaging, optoacoustics has already reached single cell detection capabilities[72] (for circulating melanoma cells).

## 10. Conclusions

With the compelling advantages of optical imaging, such as highly diverse contrast mechanisms and easy and safe usability, and with imaging performance characteristics that rival those of MRI in resolution and nuclear imaging in specificity, MSOT is expected to play a major role in biomedical research and drug discovery applications. This is because it brings a new standard of performance in small animal imaging and it can lead to significant niche clinical applications as well, especially in regimes where optical imaging is already an accepted modality, such as endoscopic applications, but possibly also in applications where deeper detection is required. As such, it can play a vital role, from monitoring dynamic phenomena noninvasively to accelerating the decision on potential drug candidates during *in vivo* screening applications and toxicology animal studies. Potentially, MSOT can play an increasingly important role through phase 0−III clinical trials by offering a method that can yield quantitative markers of treatment while it is not limited by application repetition due to cost or the use of ionizing radiation, within the application areas of the technique, as defined by its penetration ability. Therefore, it is expected that MSOT will define several new application areas and will become a method of choice in small animal and select clinical imaging applications.

## 11. Glossary

FPfluorescent protein
MRImagnetic resonance imaging
MSOTmultispectral optoacoustic tomography
NIR near infrared
SNR signal-to-noise ratio
X-ray CTX-ray computed tomography

## 12. Acknowledgments

We are thankful to many IBMI scientists for assistance and discussions in association with the imaging performance metrics reported herein. V.N. acknowledges support from the European Research Council through an Advanced Investigator Award and the Bundesministerium für Bildung and Forschung—BMBF, Germany's Federal Ministry for Education and Research Innovation in Medicine Award.

## 13. References

(1) Giepmans, B. N. G.; Adams, S. R.; Ellisman, M. H.; Tsien, R. Y. *Science* **2006**, *312*, 217.
(2) Shu, X.; Royant, A.; Lin, M.; Aguilera, T.; Lev-Ram, V.; Steinbach, P.; Tsien, R. *Science* **2009**, *324*, 804.
(3) Weissleder, R.; Pittet, M. *Nature* **2008**, *452*, 580.
(4) Achilefu, S. *Technol. Cancer Res. Treat.* **2004**, *3*, 393.
(5) Giepmans, B.; Adams, S.; Ellisman, M.; Tsien, R. *Science* **2006**, *312*, 217.
(6) Homma, R.; Baker, B. J.; Jin, L.; Garaschuk, O.; Konnerth, A.; Cohen, L. B.; Bleau, C. X.; Canepari, M.; Djurisic, M.; Zecevic, D., Wide-Field and Two-Photon Imaging of Brain Activity with Voltage- and Calcium-Sensitive Dyes. In *Methods Mol. Biol.*, Hyder, F., Ed. Humana Press: New York, 2009, 43.
(7) Wang, Y. X.; Shyy, J. Y. J.; Chien, S. *Ann. Rev. Biomed. Eng.* **2008**, *10*, 1.
(8) Watson, C.; Trainor, P.; Radziewic, T.; Pelka, G.; Zhou, S.; Parameswaran, M.; Quinlan, G.; Gordon, M.; Sturm, K.; Tam, P. *Methods Mol. Biol.* **2008**, *461*, 149.
(9) Link, A.; Jeong, K.; Georgiou, G. *Nat. Rev. Microbiol.* **2007**, *5*, 680.
(10) Malet, C.; Vallés, J.; Bou, J.; Planas, A. *J. Biotechnol.* **1996**, *48* (3), 209–19.
(11) Li, P.; Wang, C.; Shieh, D.; Wei, C.; Liao, C.; Poe, C.; Jhan, S.; Ding, A.; Wu, Y. *Opt. Express* **2008**, *16*, 18605.
(12) Rayavarapu, R.; Petersen, W.; Ungureanu, C.; Post, J.; van Leeuwen, T.; Manohar, S. *Int. J. Biomed. Imaging* **2007**, *2007*, 29817.
(13) Eghtedari, M.; Oraevsky, A.; Copland, J.; Kotov, N.; Conjusteau, A.; Motamedi, M. *Nano Lett.* **2007**, *7*, 1914.
(14) De la Zerda, A.; Zavaleta, C.; Keren, S.; Vaithilingam, S.; Bodapati, S.; Liu, Z.; Levi, J.; Smith, B.; Ma, T.; Oralkan, O.; Cheng, Z.; Chen, X.; Dai, H.; Khuri-Yakub, B.; Gambhir, S. *Nat. Nanotechnol.* **2008**, *3*, 557.
(15) Webb, R. H., *Theoretical basis of confocal microscopy*. In *Confocal Microscopy*, Elsevier Academic Press: San Diego, 1999, *307*, 3−20.
(16) Helmchen, F.; Denk, W. *Nat. Methods* **2005**, *2*, 932.
(17) Sharpe, J.; Ahlgren, U.; Perry, P.; Hill, B.; Ross, A.; Hecksher-Sorensen, J.; Baldock, R.; Davidson, D. *Science* **2002**, *296*, 541.
(18) Huisken, J.; Swoger, J.; Del Bene, F.; Wittbrodt, J.; Stelzer, E. H. K. *Science* **2004**, *305*, 1007.
(19) Ntziachristos, V.; Ripoll, J.; Wang, L. V.; Weissleder, R. *Nat. Biotechnol.* **2005**, *23*, 313.
(20) Ntziachristos, V.; Tung, C.; Bremer, C.; Weissleder, R. *Nat. Med.* **2002**, *8*, 757.
(21) Wang, X.; Pang, Y.; Ku, G.; Xie, X.; Stoica, G.; Wang, L. *Nat. Biotechnol.* **2003**, *21*, 803.
(22) Hyde, D.; de Kleine, R.; MacLaurin, S. A.; Miller, E.; Brooks, D. H.; Krucker, T.; Ntziachristos, V. *Neuroimage* **2009**, *44*, 1304.
(23) Schulz, R. B.; Ale, A.; Sarantopoulos, A.; Freyer, M.; Soehngen, E.; Zientkowska, M.; Ntziachristos, V. *IEEE Trans. Med. Imaging* **2010**, *29*, 465.
(24) Davis, S. C.; Pogue, B. W.; Springett, R.; Leussler, C.; Mazurkewitz, P.; Tuttle, S. B.; Gibbs-Strauss, S. L.; Jiang, S. S.; Dehghani, H.; Paulsen, K. D. *Rev. Sci. Instrum.* **2008**, *79*, 10.
(25) Ntziachristos, V. *Annu. Rev. Biomed. Eng.* **2006**, *8*, 1.
(26) Wang, L. V.; IEEE, J. *Sel. Top. Quantum Electron.* **2008**, *14*, 171.
(27) Wang, L. V. *Nat. Photonics* **2009**, *3*, 503.
(28) Bell, A. G. *Am. J. Sci.* **1881**, *20*, 305.
(29) Rosencwaig, A. *Science* **1973**, *181*, 657.
(30) Bowen, T.; Nasoni, L.; Pifer, A. E.; Sembroski, G. H. *Proc. IEEE Ultrasonics Symp.* **1981**, *2*, 823.
(31) Oraevsky, A. A.; Jacques, S. L.; Esenaliev, R. O.; Tittel, F. K. *Proc. SPIE* **1994**, *2134A*, 122.
(32) Kruger, R.; Kiser, W.; Reinecke, D.; Kruger, G.; Miller, K. *Mol. Imaging* **2003**, *2*, 113.
(33) Razansky, D.; Vinegoni, C.; Ntziachristos, V. *Opt. Lett.* **2007**, *32*, 2891.
(34) Li, M.-L.; Oh, J.-T.; X., X.; G, K.; Wang, W.; Li, C.; Lungu, G.; Stoica, G.; Wang, L. V. *Proc. IEEE* **2008**, *96*, 481.
(35) Razansky, D.; Distel, M.; Vinegoni, C.; Ma, R.; Perrimon, N.; Koster, R.; Ntziachristos, V. *Nat. Photonics* **2009**, *3*, 412.
(36) American Laser Institute, *American National Standards for the Safe Use of Lasers*. 2000,ANSI Z136.1.
(37) Cherry, S. *Annu. Rev. Biomed. Eng.* **2006**, *8*, 35.
(38) Zhang, H.; Maslov, K.; Stoica, G.; Wang, L. *Nat. Biotechnol.* **2006**, *24*, 848.
(39) Ma, R.; Taruttis, A.; Ntziachristos, V.; Razansky, D. *Opt. Express* **2009**, *17*, 21414.
(40) Ermilov, S.; Khamapirad, T.; Conjusteau, A.; Leonard, M.; Lacewell, R.; Mehta, K.; Miller, T.; Oraevsky, A. *J. Biomed. Opt.* **2009**, *14*, 024007.
(41) Yang, X.; Wang, L. *J. Biomed. Opt.* **2008**, *13*, 044009.
(42) Niederhauser, J.; Jaeger, M.; Lemor, R.; Weber, P.; Frenz, M. *IEEE Trans. Med. Imaging* **2005**, *24*, 436.
(43) Manohar, S.; Vaartjes, S.; van Hespen, J.; Klaase, J.; van den Engh, F.; Steenbergen, W.; van Leeuwen, T. *Opt. Express* **2007**, *15*, 12277.
(44) Wang, X.; Chamberland, D.; Jamadar, D. *Opt. Lett.* **2007**, *32*, 3002–4.
(45) Wang, B.; Yantsen, E.; Larson, T.; Karpiouk, A.; Sethuraman, S.; Su, J.; Sokolov, K.; Emelianov, S. *Nano Lett.* **2009**, *9*, 2212.
(46) Patterson, M. S.; Chance, B.; Wilson, B. C. *Appl. Opt.* **1989**, *28*, 2331.
(47) Chamberland, D. L.; Agarwal, A.; Kotov, N.; Fowlkes, J. B.; Carson, P. L.; Wang, X. *Nanotechnology* **2008**, *19*, 095101.
(48) Li, L.; Zemp, R.; Lungu, G.; Stoica, G.; Wang, L. *J. Biomed. Opt.* **2007**, *12*, 020504.
(49) Shashkov, E. V.; Everts, M.; Galanzha, E. I.; Zharov, V. P. *Nano Lett.* **2008**, *8*, 3953.
(50) Kim, S.; Lim, Y.; Soltesz, E.; De Grand, A.; Lee, J.; Nakayama, A.; Parker, J.; Mihaljevic, T.; Laurence, R.; Dor, D.; Cohn, L.; Bawendi, M.; Frangioni, J. *Nat. Biotechnol.* **2004**, *22*, 93.
(51) Bouchard, L.; Anwar, M.; Liu, G.; Hann, B.; Xie, Z.; Gray, J.; Wang, X.; Pines, A.; Chen, F. *Proc. Natl. Acad. Sci. U. S. A.* **2009**, *106*, 4085.
(52) Lam, C.; James, J.; McCluskey, R.; Arepalli, S.; Hunter, R. *Crit. Rev. Toxicol.* **2006**, *36*, 189.
(53) Zhang, E.; Laufer, J.; Pedley, R.; Beard, P. *Phys. Med. Biol.* **2009**, *54*, 1035.
(54) Hu, S.; Maslov, K.; Wang, L. *Opt. Express* **2009**, *17*, 7688.
(55) Zemp, R.; Song, L.; Bitton, R.; Shung, K.; Wang, L. *Opt. Express* **2008**, *16*, 18551.
(56) Song, L.; Kim, C.; Maslov, K.; Shung, K.; Wang, L. *Med. Phys.* **2009**, *36*, 3724.
(57) Hu, S.; Yan, P.; Maslov, K.; Lee, J.; Wang, L. *Opt. Lett.* **2009**, *34*, 3899.
(58) de la Zerda, A.; Paulus, Y. M.; Teed, R.; Bodapati, S.; Dollberg, Y.; Khuri-Yakub, B. T.; Blumenkranz, M. S.; Moshfeghi, D. M.; Gambhir, S. S. *Opt. Lett.* **2010**, *35*, 270.
(59) Kolkman, R.; Mulder, M.; Glade, C.; Steenbergen, W.; van Leeuwen, T. *Lasers Surg. Med.* **2008**, *40*, 178.
(60) Razansky, D.; Vinegoni, C.; Ntziachristos, V. *Phys. Med. Biol.* **2009**, *54*, 2769.
(61) Shah, J.; Park, S.; Aglyamov, S.; Larson, T.; Ma, L.; Sokolov, K.; Johnston, K.; Milner, T.; Emelianov, S. *J. Biomed. Opt.* **2008**, *13*, 034024.
(62) Galanzha, E.; Shashkov, E.; Kelly, T.; Kim, J.; Yang, L.; Zharov, V. *Nat. Nanotechnol.* **2009**, *4*, 855.
(63) Kim, J.; Galanzha, E.; Shashkov, E.; Moon, H.; Zharov, V. *Nat. Nanotechnol.* **2009**, *4*, 688.
(64) Fan, Y.; Mandelis, A.; Spirou, G.; Vitkin, I.; Whelan, W. *Phys. Rev. E: Stat. Nonlinear Soft Matter Phys.* **2005**, *72*, 051908.
(65) Razansky, D.; Baeten, J.; Ntziachristos, V. *Med. Phys.* **2009**, *36*, 939.
(66) Köstli, K.; Frenz, M.; Bebie, H.; Weber, H. *Phys. Med. Biol.* **2001**, *46*, 1863.
(67) Rosenthal, A.; Razansky, D.; Ntziachristos, V. *IEEE Trans. Med. Imaging* 2010, DOI: 10.1109/TMI.2010.2044584.
(68) Jetzfellner, T.; Razansky, D.; Rosenthal, A.; Schulz, R.; Englmeier, K.; Ntziachristos, V. *Appl. Phys. Lett.* **2009**, *95*, 013703.
(69) Paltauf, G.; Viator, J.; Prahl, S.; Jacques, S. *J. Acoust. Soc. Am.* **2002**, *112*, 1536.
(70) Cox, B.; Arridge, S.; Köstli, K.; Beard, P. *Appl. Opt.* **2006**, *45*, 1866.
(71) Rosenthal, A.; Razansky, D.; Ntziachristos, V. *IEEE Trans. Med. Imaging* **2009**, *28*, 1997.
(72) Galanzha, E.; Shashkov, E.; Spring, P.; Suen, J.; Zharov, V. *Cancer Res.* **2009**, *69*, 7926.

CR9002566